Band structure of superlattices of semiconductors with a degenerate valence band

L. G. Gerchikov, G. V. Rozhnov, and A. V. Subashiev

Scientific-industrial enterprise "Orion," St. Petersburg State Technical University
(Submitted 21 February 1991)
Zh. Eksp. Teor. Fiz. **101**, 143–162 (January 1992)

The miniband spectrum of semiconductor superlattices containing layers of a narrow-gap or gapless semiconductor is studied analytically in the Kane model. The dispersion equation for the spectrum of the minibands of electrons and of light and heavy holes is obtained, as well as the expressions for effective masses of minibands with allowance for carrier transformation at heterostructure interfaces. An analysis of general properties of the energy spectrum of superlattices of the GaAs–Ga_xAl_{1-x} and HgTe–CdTe type is performed. The rearrangement of the spectrum of the HgTe–CdTe superlattice with change of the structure parameters is described.

1. INTRODUCTION

Numerous experimental and theoretical studies of the band spectrum of semiconductor superlattices (SL) have shown (see Refs. 1, 2) that, when calculating the band structure, fairly good results are obtained with the help of the method of envelope functions in the multiband Kane models. This method differs, for example, from the tight-binding method, the pseudopotential method, etc. in that it is relatively simple and gives the possibility of studying analytically the general mechanisms of spectrum formation.[1)] However, in the framework of the method of envelope functions, the main results are obtained chiefly numerically, and the available analytical solutions of the problem, reducing it to the solution of a dispersion equation (DE) of the Kronig-Penney type, are found under strong simplifying assumptions[4] either in the approximation of an infinite mass of heavy holes or considering carrier motion only along the superlattice axis. The analysis thus ignores the effects of carrier transformation under reflection from the interface,[5] as well as the effects related to the surface states.[6,7] The latter effects play an important role in the formation of the SL spectrum and alter the effective masses of the carriers moving along the SL layers. Moreover, the absence of a realistic model admitting of an analytical solution makes it hardly possible to interpret and analyze many numerical results (in view of the large number of input parameters describing such structures[2]), as well as compare them with the experiment.

In the present work we have studied analytically the miniband spectrum of SL containing layers of a narrow-gap or gapless semiconductor, in the framework of the Kane model including the conduction band Γ_6 and the states of light and heavy holes of the valence band Γ_8. We show that if the warping of the hole spectrum is neglected the problem reduces to the solution of one real transcendental DE [see below Eq. (18) describing the states of light and heavy carriers in the SL arbitrarily interacting at interfaces]. We have found analytical expressions for the effective masses of the carriers near the miniband edges, when the carriers move both along the axis and along the layers of the SL. With GaAs–$Ga_xAl_{1-x}As$ and HgTe–CdTe SL as an example, we demonstrate the important role of the surface states and carrier transformation at interfaces in the formation of the SL miniband spectrum.

The DE analysis has made it possible to describe the qualitative rearrangement found earlier in numerical calculations[8,9] of the spectrum of the HgTe–CdTe type SL and in experiments.[10] This rearrangement reveals itself, in particular, in a nonmonotonic dependence of the SL band gap on the SL period, and also in the semiconductor–semimetal–indirect semiconductor transition occuring with the growth of the SL period. The results of the qualitative analysis agree with the numerical solutions of the DE obtained for the SL of the HgTe–CdTe type with different structure parameters, as well as with the results of numerical calculations of other authors, performed earlier in the tight-binding approximation.[9,11]

2. DERIVATION OF THE DISPERSION EQUATION

Consider an infinite periodic SL consisting of layers of a material *1* of thickness d_1 and layers of a material *2* of thickness d_2 with the period $d = d_1 + d_2$. To describe the SL spectrum of the carriers, we use the effective Hamiltonian of the two-band Kane model in the isotropic approximation, taking into account the states of the conduction band with symmetry Γ_6 (e), of light holes of the Γ_8 band (lh), and of heavy holes of the Γ_8 band (hh). This model allows to find the spectrum of SL including layers of narrow-gap or zero-gap semiconductors (with band inversion), in which the distance between the bands Γ_6 and Γ_8 is smaller than the spin-orbital splitting Δ of the valence band.

Let the quantization axis z be perpendicular to the plane x,y of the carrier motion, and the axis x be the superlattice axis.[12] With the axes thus chosen, the system of six Kane equations is split into two independent subsystems describing two noninteracting groups of states with definite projections of the total momentum on the quantization axis z, $(e\tfrac{1}{2}, lh -\tfrac{1}{2}, hh\ 3/2)$ and $(e -\tfrac{1}{2}, lh\ \tfrac{1}{2}, hh - 3/2)$, and differing in the sign of the wave vector projection on the y axis: $k_y \to -k_y$. In what follows we consider only the first group of states. The corresponding effective Hamiltonian is written in the form[12]

 0038-5646/92/010077-11$05.00

$$\hat{H}=\begin{pmatrix} \varepsilon_{cj} & \frac{Pk_-}{6^{1/2}} & \frac{Pk_+}{2^{1/2}} \\ \frac{Pk_+}{6^{1/2}} & \varepsilon_{vj}-\frac{\hbar^2}{2m_0}k_+(\gamma_j-\tilde{\gamma}_j)k_- & -\frac{\hbar^2}{2m_0}3^{1/2}k_+\tilde{\gamma}_jk_+ \\ \frac{Pk_-}{2^{1/2}} & -\frac{\hbar^2}{2m_0}3^{1/2}k_-\tilde{\gamma}_jk_- & \varepsilon_{vj}-\frac{\hbar^2}{2m_0}k_-(\gamma_j+\tilde{\gamma}_j)k_+ \end{pmatrix}, \tag{1}$$

where

$$k_\pm=-i\frac{\partial}{\partial x}\pm ik_y,$$

m_0 is the mass of a free electron, ε_{cj} and ε_{vj} are the positions of the edges of the bands Γ_6 and Γ_8 in the material 1 ($j=1$) and 2 ($j=2$), γ_j and $\tilde{\gamma}_j$ are modified Luttinger constants related to the interaction of the valence band Γ_8 with distant bands, and P is the Kane matrix element and is assumed to be the same for both materials. The dispersion of the electron band Γ_6 is determined mainly by the interaction with the valence band Γ_8, i.e., by the terms linear in k, therefore the contribution of the terms quadratic in kP to the electron energy in the Hamiltonian (1) is omitted. The Hamiltonian (1) turns out to be degenerate (the determinant of the matrix of the coefficients of the terms quadratic in k equals zero) and has two linearly independent eigenfunctions. This allows us to lower the dimensionality of the system $\hat{H}\Psi=\varepsilon\Psi$, excluding the electronic component of the eigenfunctions (1). As a result, instead of the 3×3 system of equations we obtain a nondegenerate 2×2 system of equations in a two-component wave function Ψ_{ν_j}

$$\sum_{\alpha,\beta=x,y}\frac{\hbar^2}{2m_0}k_\alpha D_j^{\alpha\beta}k_\beta\Psi_{\nu_j}=(\varepsilon-\varepsilon_{\nu_j})\Psi_{\nu_j}, \tag{2}$$

where $j=1,2$ is the material index, ν is the set of quantum eigenvalues, and $\alpha,\beta=x,y$ are the indices of the Cartesian coordinates. The explicit form of the matrices $D_j^{\alpha\beta}$ is given in the Appendix. The determinants of the matrices $D_j^{\alpha\beta}$ are expressed through the effective masses m_{ν_j} of light ($\nu=l$) and heavy ($\nu=h$) holes in the bulk of the materials, which are assumed to be finite:

$$|D_j^{\alpha\beta}|=\frac{m_0^2}{m_{lj}m_{hj}},$$

$$\frac{m_{hj}}{m_0}=-(\gamma_j-2\tilde{\gamma}_j)^{-1},\quad \frac{m_{lj}}{m_0}=\left[\frac{\varepsilon_P}{\varepsilon-\varepsilon_{cj}}-(\gamma_j+2\tilde{\gamma}_j)\right]^{-1}, \tag{3}$$

$$\varepsilon_P=\frac{4m_0P^2}{3\hbar^2}.$$

The dependence of m_{lj} on the energy ε reflects the nonparabolicity of the bands of light carriers.

The eigenfunctions of the system (2) in the bulk of the materials $j=1,2$ for a given energy ε and a projection $k_y=K$ of the wave vector on the layer plane have the following form for light carriers:

$$\Psi_{lj}^{\pm}=\begin{pmatrix} \pm k_{lj}+iK \\ 3^{1/2}(\pm k_{lj}-iK) \end{pmatrix}\exp[i(Ky\pm k_{lj}x)], \tag{4}$$

and for heavy carriers:

$$\Psi_{hj}^{\pm}=\begin{pmatrix} 3^{1/2}(\pm k_{hj}+iK) \\ -(\pm k_{hj}-iK) \end{pmatrix}\exp[i(Ky\pm k_{hj}x)], \tag{5}$$

where k_{ν_j} is the projection of the wave vector of the carriers of the type $\nu=l,h$ in the materials $j=1,2$ on the direction of the SL axis:

$$k_{\nu j}=\left[\frac{2m_{\nu j}}{\hbar^2}(\varepsilon-\varepsilon_{\nu j})-K^2\right]^{1/2}, \tag{6}$$

where the masses m_{ν_j} are defined in (3). In (6) we choose the branch of the root for which $\mathrm{Re}\,k_{\nu_j}\geqslant0$ ($\mathrm{Im}\,k_{\nu_j}\geqslant0$).

In a superlattice the projection K of the wave vector on the plane of the layers is conserved, therefore the general solution (2) for the wave function $\Psi(x)$ in each layer is a linear superposition of the functions (4) and (5):

$$\Psi(x)=C_{1j}\Psi_{hj}^{+}+C_{2j}\Psi_{hj}^{-}+C_{3j}\Psi_{lj}^{+}+C_{4j}\Psi_{lj}^{-}, \tag{7}$$

where C_{lj} ($l=1,2,3,4, j=1,2$) are arbitrary constants.

The boundary conditions at the interface between materials 1 and 2, e.g., at $x=0$, determine a linear relationship between the amplitude coefficients C_{lj} from Eq. (7), of the form (see the Appendix)

$$C_{l1}=\sum_{m=1}^{4}R_{lm}C_{m2}. \tag{8}$$

A similar boundary condition holds also at the neighboring interface at $x=d_1$. In writing it down one has to allow for the phase variation in each term in Eq. (7) and for the periodic boundary condition

$$\Psi(x+d)=e^{iQd}\Psi(x), \tag{9}$$

where $\hbar Q$ is the projection of the carrier quasimomentum on the SL axis. As a result, we have

$$\sum_{m=1}^{4}(U_1)_{lm}C_{m1}=e^{iQd}\sum_{m,n=1}^{4}R_{lm}(U_2^{-1})_{mn}C_{n2}, \tag{10}$$

where the matrix U_j gives the variation of the phase of the components of the wave function (7) in the layers:

$$U_j=\begin{pmatrix} \exp(ik_{hj}d_j) & 0 & 0 & 0 \\ 0 & \exp(-ik_{hj}d_j) & 0 & 0 \\ 0 & 0 & \exp(ik_{lj}d_j) & 0 \\ 0 & 0 & 0 & \exp(-ik_{lj}d_j) \end{pmatrix}. \tag{11}$$

From (8) and (10) we obtain a homogeneous system of linear equations in the amplitude coefficients C_{lj} of the superposition (7):

$$\sum_{m=1}^{4} (Ie^{iQd}-T_j)_{lm} C_{mj} = 0, \quad l=1,2,3,4, \quad j=1,2, \tag{12}$$

where T_j is the transfer matrix of the superlattice:

$$T_1=RU_2R^{-1}U_1, \quad T_2=U_2R^{-1}U_1R. \tag{13}$$

The dispersion equation to find the SL spectrum is obtained by equating the determinant of the system (12) to zero:

$$|Ie^{iQd}-T_j|=0. \tag{14}$$

The equation (14) is the same for $j = 1,2$, therefore we omit this index below, $T_j = T$. The matrix DE (14) is an equation of fourth degree in the eigenvalues $\exp(iQd)$ of the matrix T and is typical of the problem of propagation of two types of interacting waves in multilayer structures.[13] In Ref. 13 the equation of the type (14) is reduced to a transcendental one in a linear approximation in the off-diagonal elements of the matrix T, valid under the condition of weak interaction between the waves. It will be shown below that the SL symmetry allows us to reduce the matrix equation (14) to a real transcendental one, given an arbitrary interaction between the waves. For that we rewrite the left-hand side of Eq. (14) as a power series in e^{iQd}:

$$e^{4iQd}-S_1e^{3iQd}+S_2e^{2iQd}-S_3e^{iQd}+S_4=0. \tag{15}$$

The expansion coefficients $S_n(\varepsilon,K)$, $n = 1,2,3,4$, are the sums of all the principal minors of the matrix T of order n.[14] In particular, $S_1 = \mathrm{Tr}T$, $S_4 = |T| = 1$. The last expression follows from (11) and (13). Moreover, since $|T| = 1$, $S_3 = \mathrm{Tr}(T^{-1})$; from this taking into account Eqs. (11) and (13), we have $S_3 = S_1(-d_1, -d_2)$. In the structures considered, having a symmetry plane perpendicular to the SL axis, $S_1(d_1,d_2) = S_1(-d_1, -d_2)$, which gives $S_1 = S_3$. Thus, in the general case the DE (15) reduces to

$$\cos 2Qd - S_1 \cos Qd + {}^1/_2 S_2 = 0. \tag{16}$$

In the simplest case of the propagation of waves which do not experience mutual transformations at the interfaces (in the problem of the SL carrier spectrum this takes place for $K = 0$), the matrix T is block-diagonal:

$$T = \begin{pmatrix} T_h & 0 \\ 0 & T_l \end{pmatrix}.$$

The coefficients S_1 and S_2 given that $|T_h| = |T_l| = 1$ are easily expressed through the diagonal elements of the matrix $T_{h,l}$ and Eq. (16) reduces to two DE for noninteracting waves:

$$(\cos Qd - {}^1/_2 \,\mathrm{Sp}\, T_h)(\cos Qd - {}^1/_2 \,\mathrm{Sp}\, T_l) = 0. \tag{17}$$

In the general case of interacting carriers, straightforward calculations of the coefficients S_1 and S_2 and their expression through the elements of the matrices R and U_j reduces DE (16) to the form

$$(\cos Qd - G_h)(\cos Qd - G_l) = s_2 - s_1 \cos Qd, \tag{18}$$

where

$$G_v(\varepsilon, K) = \cos k_{v1}d_1 \cos k_{v2}d_2 - \frac{x_{v1}^2+x_{v2}^2+g^2}{2x_{v1}x_{v2}} \sin k_{v1}d_1 \sin k_{v2}d_2, \tag{19}$$

$$s_1(\varepsilon, K) = \frac{3}{2} g^2 \left(\frac{\sin k_{h1}d_1}{x_{h1}} \frac{\sin k_{l2}d_2}{x_{l2}} + \frac{\sin k_{l1}d_1}{x_{l1}} \frac{\sin k_{h2}d_2}{x_{h2}} \right),$$

$$\begin{aligned} s_2(\varepsilon, K) = \frac{3}{2} g^2 \Bigg\{ & \left(\cos k_{h1}d_1 \frac{\sin k_{h2}d_2}{x_{h2}} + \frac{\sin k_{h1}d_1}{x_{h1}} \cos k_{h2}d_2 \right) \\ & \times \left(\cos k_{l1}d_1 \frac{\sin k_{l2}d_2}{x_{l2}} + \frac{\sin k_{l1}d_1}{x_{l1}} \cos k_{l2}d_2 \right) \\ & - \left(\frac{\sin k_{l1}d_1}{x_{l1}} \frac{\sin k_{h1}d_1}{x_{h1}} \right. \\ & \left. + \frac{\sin k_{l2}d_2}{x_{l2}} \frac{\sin k_{h2}d_2}{x_{h2}} \right) \\ & - \frac{5}{2} g^2 \frac{\sin k_{l1}d_1}{x_{l1}} \frac{\sin k_{l2}d_2}{x_{l2}} \frac{\sin k_{h1}d_1}{x_{h1}} \frac{\sin k_{h2}d_2}{x_{h2}} \Bigg\}. \end{aligned} \tag{20}$$

Here

$$g = K\Lambda/2(\varepsilon-\varepsilon_{v1})(\varepsilon-\varepsilon_{v2}), \quad x_{vj} = k_{vj}/(\varepsilon-\varepsilon_{vj}), \quad \Lambda = \varepsilon_{v1}-\varepsilon_{v2}$$

where Λ is the valence band discontinuity at the interface. The left-hand side of Eq. (18) contains factors describing independent quantization of light and heavy carriers, and the right-hand side, connected with interaction, is proportional to the factor g^2 and contains only the cross terms in the indices of the light and heavy carriers.

In the limiting case, when one of the materials, e.g., the material 2, is a low-transparency barrier for all the carriers, so that $|k_{v2}|d \gg 1$, Eq. (18) reduces to the equation of size quantization of the carriers in a solitary quantum well[7]

$$\begin{aligned} & \left(\cos k_{h1}d_1 - i \frac{x_{h1}^2+x_{h2}^2+g^2}{2x_{h1}x_{h2}} \sin k_{h1}d_1 \right) \\ & \times \left(\cos k_{l1}d_1 - i \frac{x_{l1}^2+x_{l2}^2+g^2}{2x_{l1}x_{l2}} \sin k_{l1}d_1 \right) \\ & = \frac{3}{2} \frac{g^2}{x_{h2}x_{l2}} \Bigg[1 - \left(\cos k_{h1}d_1 - i \frac{x_{h2}}{x_{h1}} \sin k_{h1}d_1 \right) \\ & \times \left(\cos k_{l1}d_1 - i \frac{x_{l2}}{x_{l1}} \sin k_{l1}d_1 \right) \\ & + \frac{5}{2} \frac{g^2}{x_{h1}x_{l1}} \sin k_{h1}d_1 \sin k_{l1}d_1 \Bigg]. \end{aligned} \tag{21}$$

An analysis of this equation is carried out in Ref. 7. If we consider besides the well to be infinitely wide, so that $|k_{v1}|d_1 \gg 1$, Eq. (21) reduces to the DE of surface states of a single hetero-junction:

$$(x_{h1}+x_{h2}+ig)(x_{l1}+x_{l2}-ig)+3g^2=0. \tag{22}$$

These surface states have been discussed in Refs. 5 and 6.

3. EFFECTIVE MASSES OF THE CARRIERS

The analysis of DE (18) becomes simpler near the miniband edges for $K=0$ and $Q=0,\ \pi/d$, since the DE (18) breaks up at $K=0$ into independent equations for light and heavy carriers

$$\cos Qd=G_\nu(\varepsilon,\ 0), \tag{23}$$

where $G_\nu(\varepsilon,0)$ is given by (19) for $K=0$. For $Q=0$ and and $Q=\pi/d$ Eq. (23) gives two pairs of independent equations

$$\Phi_{\alpha\beta}{}^{\nu}(\varepsilon,\ d_1,\ d_2)=0 \tag{24}$$

for each type of carriers, $\nu=l,h$, where

$$\Phi_{\alpha\beta}{}^{\nu}=\alpha x_{\nu 1}\left[\operatorname{ctg}\frac{k_{\nu 1}d_1}{2}\right]^{\alpha}+\beta x_{\nu 2}\left[\operatorname{ctg}\frac{k_{\nu 2}d_2}{2}\right]^{\beta}. \tag{25}$$

In Eqs. (24) and (25) $\alpha=\pm 1$ and $\beta=\alpha e^{iQd}$. The splitting of Eq. (18) into four independent equations is due to an extra quantum number, the parity of states, appearing for $Q=0,\ \pi/d$. The index α indicates either even ($\alpha=+1$) or odd ($\alpha=-1$) parity of states in the material 1, and β labels even or odd parity of states in the material 2. The center of the Brillouin zone, $Q=0$, corresponds to the case $\alpha=\beta$, while the edge $Q=\pi/d$ to the case $\alpha=-\beta$. Equation (24) solved for ε gives the position of the miniband edges $\varepsilon^{\nu}_{\alpha\beta,n}(d_1,d_2)$, where n is the miniband number ($n=1,2,3,\ldots$).[2)] Equation (23) leads to expressions for the effective masses $m^{\nu\parallel}_{\alpha\beta,n}$ of the carriers moving along the SL axis and belonging to different minibands:

$$m^{\nu\parallel}_{\alpha\beta,n}=-\left[m_{\nu 1}Z_{\nu 1}{}^{\alpha}-\frac{dm_{\nu 1}}{d\varepsilon}(\varepsilon-\varepsilon_{\nu 1})Z_{\nu 1}{}^{\bar\alpha}-m_{\nu 2}Z_{\nu 2}{}^{\beta}+\frac{dm_{\nu 2}}{d\varepsilon}(\varepsilon-\varepsilon_{\nu 2})Z_{\nu 2}{}^{\bar\beta}\right]\times\frac{(\alpha\cos k_{\nu 1}d_1-\beta\cos k_{\nu 2}d_2)}{d^2}, \tag{26}$$

where

$$Z^{\pm}_{\nu_j}=\frac{1}{k_{\nu j}{}^2}\left(1\pm\frac{k_{\nu j}d_j}{\sin k_{\nu j}d_j}\right), \tag{27}$$

the left-hand side of Eq. (26) being calculated for the miniband edges, when $\varepsilon=\varepsilon^{\nu}_{\alpha\beta,n}$. To calculate the effective masses $m^{\nu\perp}_{\alpha\beta,n}$ near the miniband edges $\varepsilon^{\nu}_{\alpha\beta,n}$, when the carriers move along the SL layers, one has to use the initial DE (18) and expand it in powers of K. Thus, we obtain

$$m^{\nu\perp}_{\alpha\beta,n}=-\frac{m_{\nu 1}Z_{\nu 1}{}^{\alpha}-(dm_{\nu 1}/d\varepsilon)(\varepsilon-\varepsilon_{\nu 1})Z_{\nu 1}{}^{\bar\alpha}-m_{\nu 2}Z_{\nu 2}{}^{\beta}+(dm_{\nu 2}/d\varepsilon)(\varepsilon-\varepsilon_{\nu 2})Z_{\nu 2}{}^{\bar\beta}}{Z^{a}_{\nu 1}-Z^{\bar\beta}_{\nu 2}+(\lambda^2/2\alpha x_{\nu 1})\operatorname{tg}^{\alpha}(k_{\nu 1}d_1/2)(1/\Phi_{\bar\alpha\bar\beta}{}^{\nu}+3/\Phi_{\bar\alpha\bar\beta}{}^{\bar\nu})}, \tag{28}$$

where

$$\lambda=\frac{\Lambda}{(\varepsilon-\varepsilon_{\nu 1})(\varepsilon-\varepsilon_{\nu 2})},$$

$\nu=l,h$; $\alpha,\beta=\pm 1$, and $\bar\nu,\bar\alpha,\bar\beta$ are the indices complementary to ν,α,β and having opposite signs. For example, if $\nu=h,\ \alpha=+1,\ \beta=-1$, then $\bar\nu=l,\ \bar\alpha=-1,\ \bar\beta=+1$, etc. The right-hand side of (28) is calculated for the band edge, when $\varepsilon=\varepsilon^{\nu}_{\alpha\beta,n}$. The important distinction between the formula (28) for the effective masses of the carriers moving along the SL layers and the formula (26) is the appearance in (28) of terms depending on the parameters of the carriers of the other type, owing exclusively to the effects of the carrier transformation at the interfaces. As follows from (28), the minibands corresponding to carriers of different type and opposite parity interact strongly.

Upon intersection of the miniband edges, the masses of motion along the SL layers vanish, and the quadratic dispersion law is replaced by a linear one. For the masses of motion along the SL axis a similar situation arises when there is an intersection of the edges of minibands corresponding to carriers of one type but opposite parity. A more detailed analysis of the carrier mass dependence on the parameters of the SL layers will be carried out in Sec. 5.

4. GENERAL PROPERTIES OF THE ENERGY SPECTRUM FOR A SMALL RATIO OF THE MASSES OF LIGHT AND HEAVY CARRIERS

The structure of the carrier energy spectrum in the SL corresponding to the DE (18) can be qualitatively analyzed in the general case for a small but finite ratio of the masses of light and heavy carriers:

$$\beta=m_l/m_h\ll 1.$$

Since the masses differ so much, all the solutions of Eq. (18) can be separated into minibands with a strong dispersion, i.e., the minibands of electrons and light holes, and minibands with a weak dispersion, corresponding to heavy holes. Then we can consider their mutual influence which can be weak in a certain range of the energy ε and momenta K.

To be specific, let us assume that the band gap in the material 1 is smaller than in the material 2, the layer of the material 1 being a potential well for both the electrons and holes. Consider first the range of small values of the momentum of the carrier motion in the layer plane, $\hbar^2K^2/m_l\leqslant|\varepsilon-\varepsilon_{v1}|$ (range I), in which there are minibands of both light and heavy carriers. In this range, generally speaking, $k_{l1}\sim K$, whereas $k_{h1}\gg K$, i.e., heavy holes move practically along the normal to the interfaces, hindering the transformation of heavy carriers into light ones and vice versa. In fact, in the range I the right-hand side of the DE (18) is of order $K/k_{h1}\sim\beta^{1/2}\ll 1$. Therefore in the range I, to the zeroth order in β, Eq. (18) breaks up into two equations of independent quantization of light and heavy carriers, of the Kronig–Penney DE type:

$$\cos Qd=G_\nu(\varepsilon,\ K),\quad \nu=l,\ h. \tag{29}$$

Each of these equations describes the propagation of only one type of carrier in the SL. Equation (29) for the independent quantization of light carriers at $\gamma=\tilde\gamma=0$ coincides

with the DE found in the model with an infinitely large mass of heavy holes.[4] The Hamiltonian (1) turns out to be degenerate for $\gamma = \tilde{\gamma} = 0$ and gives the propagation of only light carriers, so that the problem reduces to a "single-wave" one. For $\nu = h$ the g^2 term in the right-hand side of Eq. (29) is small, and should be neglected. In this case Eq. (29) for heavy holes does not differ from the DE for a simple particle of mass m_h in a periodic potential, whereas for light particles there appear some distinctions related to the presence of special boundary states at some interfaces,[6] the most important of which, from the point of view of the SL spectrum, is the one leaving the top of the valence band of the narrow-gap material 1, when $K = 0$, and having a mass $4/3m_{l1}$ for $\beta \ll 1$.[5] The light-carrier spectrum peculiarities related to boundary states have been discussed at length in Ref. 7 for the case of the quantum-well spectrum. The main results obtained there apply also to the SL spectrum.

Allowance for the right-hand side of the DE (18) for the minibands of light and heavy holes transforms, the intersections of the hole minibands for finite K into quasi-intersections, and the minibands of light and heavy particles of opposite parity and close values of $\varepsilon^{\nu}_{\alpha\beta,n}$ repel each other in the vicinity of $K = 0$. The width of the quasi-intersection region can be estimated using the right-hand side of Eq. (18), as had been done in Ref. 7 for a solitary quantum well. This region is narrow in the parameter $(\hbar^2 K^2/m_l \Lambda)^{1/2}$, when the minibands of light and heavy holes of the same parity cross each other. In the general case, the levels repel each other to a distance of the same order as the distance between the minibands of heavy holes, so that the spectrum in the region of the miniband interaction differs essentially from the one corresponding to the independent quantization of light and heavy holes. In particular, if for $K = 0$ the energies $\varepsilon^{l}_{\alpha\beta,n}$ and $\varepsilon^{h}_{\bar{\alpha}\bar{\beta},m}$ of a pair of minibands are close to each other, the effective masses of the carrier motion along the SL layers, due to the miniband repulsion, become small, opposite in sign and close in value.

A repulsion of the same kind between the levels manifests itself, when the boundary state of light carriers, leaving the top of the valence band of the narrow-gap material 1 at $K = 0$, interacts with nearby levels of heavy holes.[7] As a result of this interaction the mass of heavy holes corresponding to odd minibands turns out to be of order m_l for the motion along the SL layers.

Thus, in the whole range of coexistence of the minibands of light and heavy holes,

$$K \ll \frac{(m_l|\varepsilon - \varepsilon_{v1}|)^{1/2}}{\hbar}$$

the SL spectrum is a system of levels of light and heavy holes repelling each other. In a wider range

$$K \sim \frac{(m_h|\varepsilon - \varepsilon_{v1}|)^{1/2}}{\hbar}$$

(range II) the waves of light holes are exponentially damped in both materials. As a result, for $K \sim 1/d_1$ and $1/d_2$, light holes do not essentially affect the states of heavy holes, so that with increasing K the minibands of heavy holes become parabolic asymptotes with a mass of motion along the SL layers close to the volume mass m_{h1} of heavy holes.

In the region of electron minibands $\varepsilon > \varepsilon_{v1}, \varepsilon_{c1}$, distant from the minibands of heavy holes, the corrections to the spectrum of the DE (29) for the carrier transformation at the interfaces are negligible. In this energy range, for materials with

$$\varepsilon_g = \varepsilon_{c1} - \varepsilon_{v1} \gtrsim \Delta$$

the influence of the band Γ_7 split off due to the spin-orbit coupling becomes more important,[6] as well as the interaction with distant bands, which limits the range of use of the DE (18). Nevertheless, the spectrum of electron minibands can be analytically described for $\Delta \lesssim \varepsilon_g$ as well. Due to a weak influence of heavy holes, we can set the mass of heavy holes in the Hamiltonian (1) equal to infinity, having included, however, the terms of the interaction of the bands Γ_6 and Γ_7 linear in kP, as well as in the electron energy, the term quadratic in k allowing for the interaction of the conduction band with all the distant bands, except the valence one. Taking this interaction into account still leaves the problem in the framework of the single-wave approximation, and the system $H\Psi = \varepsilon\Psi$ reduces to a scalar equation for the electronic component of the wave function

$$\sum_{\alpha,\beta=x,y} \frac{\hbar^2}{2m_0} k_\alpha D_j^{\alpha\beta} k_\beta \Psi_j^{(e)} = (\varepsilon - \varepsilon_{cj}) \Psi_j^{(e)}, \tag{30}$$

where

$$D_j^{xx} = D_j^{yy} = \frac{3}{2} \frac{\varepsilon_P(\varepsilon - \varepsilon_{vj} + {}^2/_3\Delta_j)}{(\varepsilon - \varepsilon_{vj})(\varepsilon - \varepsilon_{vj} + \Delta_j)} + \frac{1}{m_j^*},$$
$$D_j^{xy} = -D_j^{yx} = -i \frac{\varepsilon_P \Delta_j}{2(\varepsilon - \varepsilon_{vj})(\varepsilon - \varepsilon_{vj} + \Delta_j)}. \tag{31}$$

As follows from Eqs. (30) and (31), the off-diagonal components $D_j^{xy} = -D_j^{yx}$, describing the relation between the motion along and across to the SL axis, are connected with the spin-orbit splitting of the valence band $[D_j^{xy} \sim \Delta/(\varepsilon_g + \Delta)]$ and give a nonzero contribution to (30) only near the interfaces. Correspondingly, the contribution of distant bands is allowed for in (31) by the term $(m_j^*)^{-1}$ in the diagonal components $D_j^{\alpha\alpha}$, whereas their contribution to the nondiagonal components is omitted.

Solving Eq. (30) for the SL, we obtain a DE of the form (29), where G_ν ($\nu = l$) is given by (19) with the parameters

$$x_{lj} = k_{lj} D_j^{xx}/\varepsilon_P,$$
$$g = iK(D_1^{xy} - D_2^{xy})/\varepsilon_P. \tag{32}$$

The normal components of the electronic wave vectors should be found from the bulk dispersion law for the materials $j = 1, 2$:

$$k_{lj} = \left[\frac{2m_0}{\hbar^2 D_j^{xx}}(\varepsilon - \varepsilon_{cj}) - K^2\right]^{1/2}.$$

For the hole minibands the effect of the split-off band Γ_7 is small, if $|\varepsilon - \varepsilon_{v1}| \ll \Delta$. Therefore, in the case of the SL of semiconductors, belonging to the fourth group, or of the A_3B_5 type with small Δ the results are valid only for the first minibands of heavy holes, if the hole wells are not very narrow. The masses of these minibands are given, to a sufficient accuracy, by the expressions (26)–(28). Furthermore, since the interaction between light and heavy carriers is absent, when they move along the SL axis, (with the band Γ_7 taken

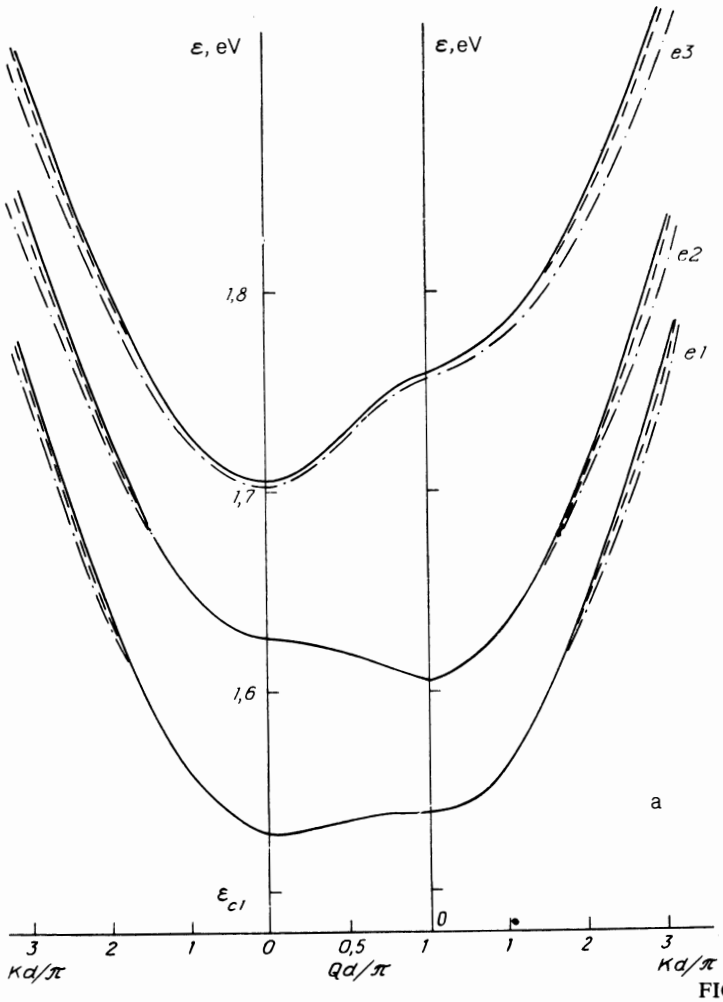

FIG. 1. The energy spectrum of electron (a) and hole (b) minibands in the GaAs–$Ga_{0.7}Al_{0.3}As$ SL with (solid lines) and without (dashed lines) the effects of carrier transformation at the interfaces. Dash-dot lines show the electronic spectrum in the single wave approximation, the effect of the band Γ_7 taken into account.

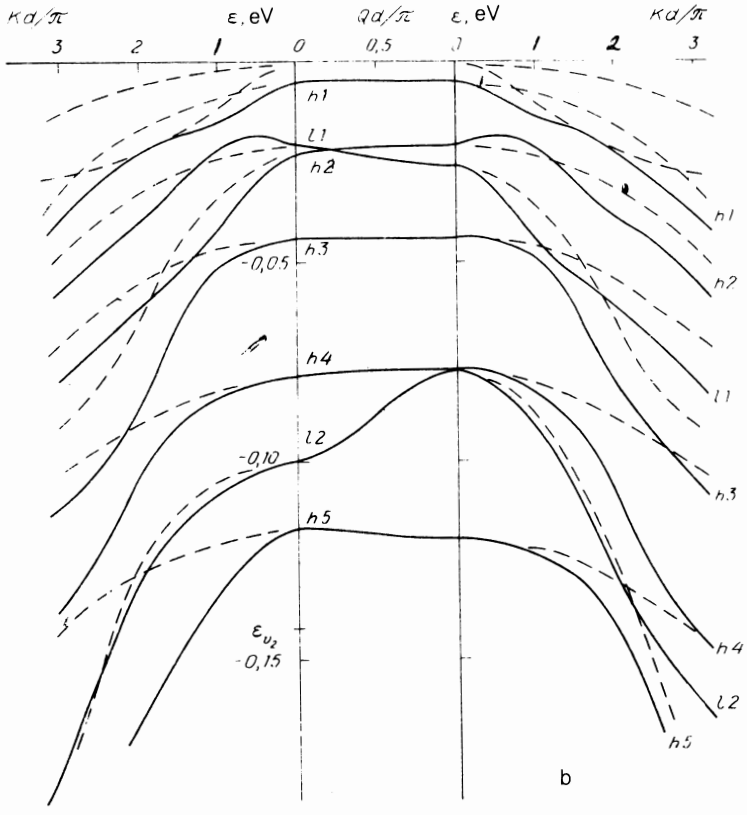

into account or not), the spectrum of heavy minibands for $K = 0$ does not depend on Δ, and the spectrum of light holes for $K = 0$ is given in the single-wave approximation by a DE of the form (29).

These general considerations are illustrated by Fig. 1. It shows the dispersion laws of the minibands $\varepsilon_n^{\nu}(Q,K)$ for the GaAs–$Ga_{0.7}Al_{0.3}As$ SL found as a numerical solution of Eq. (18), as well as the solutions of Eqs. (29) of independent quantization of heavy and light carriers with or without allowance for the band split off by the spin-orbit coupling. The superlattice parameters are $d_1 = 100$ Å and $d_2 = 40$ Å; the parameters of the materials coincide with those given in Ref. 15. Here and below the origin coincides with the edge of the valence band of the narrow-gap material: $\varepsilon_{v1} = 0$. Attention is called, first, to the weak effect of the interaction of heavy and light holes on electronic minibands and to a more pronounced effect of the band Γ_7; second, to a considerable reduction of the mass $m_1^{h\perp}$ of the miniband h 1; third, to the repulsion of the minibands l 1 and h 2 for small K, reversing the sign of the mass $m_n^{\nu\perp}$ of the upper band; fourth, to heavy asymptotes of the minibands in the range $K > (m_l|\varepsilon - \varepsilon_{v1}|)^{1/2}/\hbar$; and fifth, to sufficiently narrow regions of the miniband quasi-intersection. The observed picture fully corresponds to the qualitative analysis of the DE (18) given above.

5. REARRANGEMENT OF THE BAND STRUCTURE OF A SUPERLATTICE CONTAINING LAYERS OF A NARROW-GAP SEMICONDUCTOR, FOLLOWING A CHANGE IN SUPERLATTICE PARAMETERS

The band structure of an SL containing layers of a semiconductor with band inversion, e.g., HgTe–CdTe, has an extra distinction connected with the existence of a boundary state on an isolated interface of such materials in the energy range $\varepsilon_{v2} < \varepsilon < \varepsilon_{v1}$ (Ref. 6). In the SL the position of these energy levels strongly depends on the structure parameters d_1 and d_2, leading, as shown below, to a considerable rearrangement of the energy spectrum. Below we analyze the spectrum of such an SL in more detail.

The position of the edges of the minibands $\varepsilon_{\alpha\beta,n}^{\nu}$ for $K = 0$ and $Q = 0$, π/d and various d_1 and d_2 is determined by the solution of the transcendental equations (24). The dependence of $\varepsilon_{\alpha\beta,n}^{\nu}(d_1,d_2)$ on the potential well width d_1 for a fixed value of the potential barrier width d_2 in the HgTe–CdTe SL is shown in Fig. 2. The results of the numerical solution of Eqs. (24) are listed for $d_2 = 36$ Å and $\Lambda = 350$ meV. The values of other parameters corresponding to $T = 4$ K are taken from Ref. 16. For heavy holes Eqs. (24) give the usual sequence of minibands $\varepsilon_{\alpha\beta,n}^{h}$, $n = 1,2,3,...$, stemming from the levels ε_n^h, $n = 1,2,3...$ of size quantization in isolated quantum wells. For light particles

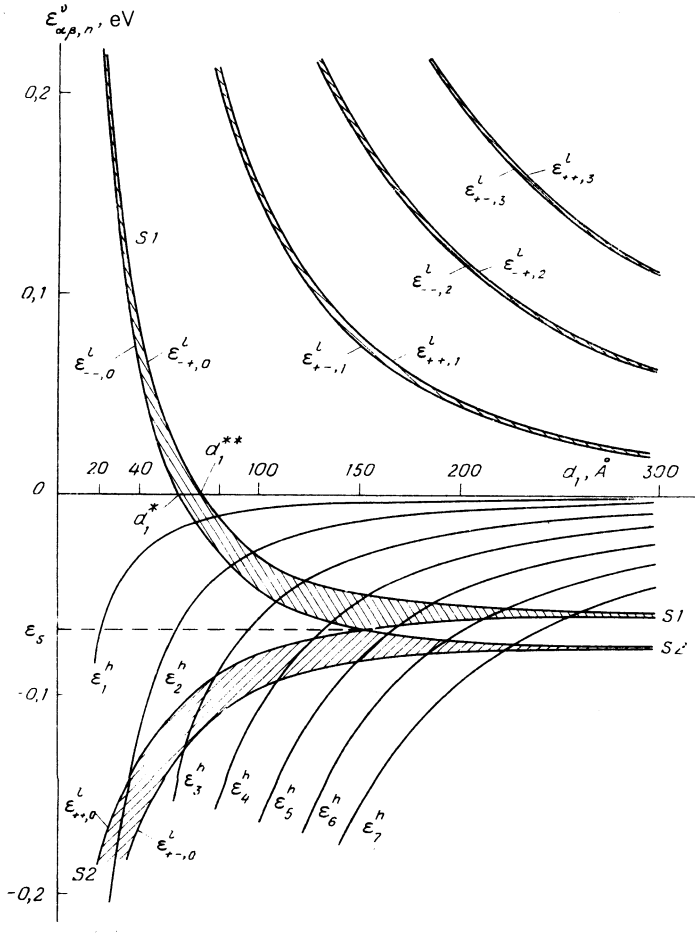

FIG. 2. The position of the edges of the minibands $\varepsilon_{\alpha\beta,n}^{\nu}$ for the HgTe–CdTe SL versus the width d_1 of the HgTe layers for $d_{CdTe} = 36$ Å, $\Lambda = 0.35$ eV, $T = 4$ K. The shaded regions are the states of the continuum spectrum for $K = 0$ and $0 \leqslant Q \leqslant \pi/d$.

Eqs. (24) give the energies $\varepsilon^{l}_{\alpha\beta,n}$ $n = 1,2,3...$, of the edges of electronic minibands in the range $\varepsilon > \varepsilon_{v1}$ and the energies of the light-hole minibands in the range $\varepsilon < \max(\varepsilon_{v2},\varepsilon_{c1})$ (they are not shown in Fig. 2). Also, Eqs. (24) have extra solutions $\varepsilon^{l}_{\alpha\beta,0}$ for $\nu = l$, which for sufficiently large widths d_1 and d_2 lie in the interval $\max(\varepsilon_{v2},\varepsilon_{c1}) < \varepsilon < \varepsilon_{v1}$ and have imaginary values of k_{l1} and k_{l2}. For

$$\exp(-|k_{lj}d_j|) \ll 1$$

these solutions reduce to the solution of Eq. (22) for a boundary state of an isolated HgTe–CdTe heterojunction at $K = 0$:

$$\varepsilon_S = \varepsilon_{v1} - \frac{m_{l1}(\varepsilon_S)\Lambda}{m_{l1}(\varepsilon_S) + |m_{l2}(\varepsilon_S)|}.$$

For finite values of the barrier and well widths, $|k_{l1}d_1| > |k_{l2}d_2| \gg 1$ the level ε_S is split into two sublevels which broaden to minibands. The upper one, $S1$, corresponds to even states in individual potential barriers, and the lower $S2$ to odd states (see Fig. 2).

For

$$d_1 = \frac{|m_{l2}|}{m_{l1}} d_2, \qquad \varepsilon = \varepsilon_S$$

the lower edge of the miniband $S1$ crosses the upper edge of the miniband $S2$. Given further decrease of d_1, the lower edge of the upper miniband $S1$ corresponds to an antisymmetric state in the region of potential wells and barriers, and the upper edge of the miniband $S2$ to a symmetric state. With d_1 decreasing, the miniband $S1$ crosses the edge of the valence band ε_{v1} and passes to the region of electronic states. For the lower edge of the miniband $S1(Q = 0)$ this occurs, when the layer thickness of material 1 is $d_1 = d_1^*$ $(Q = 0) = d_1^*$:

$$d_1^*(Q=0) = d_0 \operatorname{th}\frac{\chi_{l2}d_2}{2}, \tag{33}$$

and for the upper edge $S1$ $(Q = \pi/d)$, when $d_1 = d_1^*$ $(Q = \pi/d) = d_1^{**}$:

$$d_1^*(Q=\pi/d) = d_0 \operatorname{cth}(\chi_{l2}d_2/2), \tag{34}$$

where

$$d_0 = \frac{\hbar}{m_{l1}(\varepsilon_{v1})}\left(\frac{2|m_{l2}(\varepsilon_{v1})|}{\Lambda}\right)^{1/2},$$
$$\chi_{l2} = \frac{(2|m_{l2}(\varepsilon_{v1})|\Lambda)^{1/2}}{\hbar}.$$

It is important that the position of the miniband $S1$ strongly changes with the layer thickness, crossing many times the minibands of heavy holes. For a fixed value of Q and $K = 0$ the intersection with the miniband hn occurs for a certain $d_1 = d_{1,n}(Q)$, the analytical expression for which can be obtained from (23) at $\beta = m_{l1}/m_{h1} \ll 1$:

$$d_{1,n}(Q) = d_1^*(Q)\left\{1+\beta\frac{(\pi n)^2}{4}\left[\frac{1}{3}+\frac{\sin^2 Qd}{(\operatorname{ch}\chi_{l2}d_2-\cos Qd)^2}\right.\right.$$
$$\left.+\frac{1}{2}\frac{m_{l1}}{m_{l2}}\left(\frac{\operatorname{sh}\chi_{l2}d_2}{\operatorname{ch}\chi_{l2}d_2-\cos Qd}\right)^2\right]$$
$$\times\left(1+\frac{2}{m_{l1}}\frac{dm_{l1}}{d\varepsilon}\Lambda-\frac{1}{m_{l2}}\frac{dm_{l2}}{d\varepsilon}\Lambda\right.$$
$$\left.\left.-\left(1+\frac{1}{m_{l2}}\frac{dm_{l2}}{d\varepsilon}\Lambda\right)\frac{\chi_{l2}d_2(\operatorname{ch}\chi_{l2}d_2\cos Qd-1)}{\operatorname{sh}\chi_{l2}d_2(\operatorname{ch}\chi_{l2}d_2-\cos Qd)}\right)\right]\right\}, \tag{35}$$

where

$$d_1^*(Q) = d_0\frac{\operatorname{ch}\chi_{l2}d_2-\cos Qd}{\operatorname{sh}\chi_{l2}d_2}.$$

Near the point of the intersection of the miniband edges the minibands repel each other, their dispersion in the layer plane increasing. In accordance with (28), the odd miniband $S1$ interacts intensely with even bands hn. In this region Eq. (18) yields the following expressions for the miniband masses ($\beta \ll 1$):

$$m_n^{h\perp}(Q) = m_{l1}\frac{(\pi n)^2}{6}\frac{d_1-d_{1,n}(Q)}{d_1}, \qquad n=1,3,5\ldots,$$
$$m_{S1}^{l\perp}(Q) = m_{l1}\frac{d_1-d_1^*(Q)}{3d_1}\frac{4x}{\operatorname{tg}x-x}, \tag{36}$$
$$x = \frac{\pi}{2}\left[\frac{d_1-d_1^*(Q)}{d_{1,1}(Q)-d_1^*(Q)}\right]^{1/2}.$$

The values of $m_n^{h\perp}(Q)$ and $m_{S1}^{l\perp}(Q)$ corresponding to the band edges for $Q = 0$, π/d can be obtained from the formula (28), since

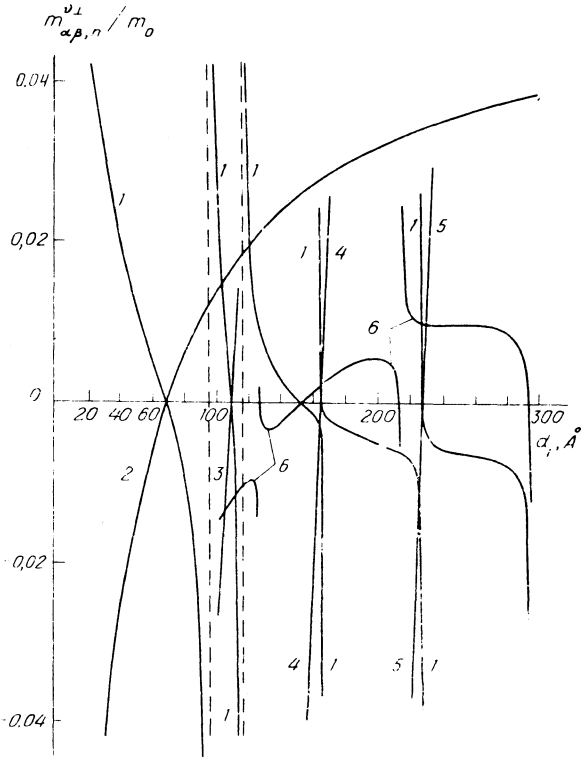

FIG. 3. The dependence of masses $m^{\nu\perp}_{\alpha\beta,n}$ along the HgTe–CdTe SL layers on the width of the HgTe layers for the SL parameters of Fig. 2. The minibands have the following indices: *1*—$\nu = l$, $\alpha = \beta = -1$, $n = 0$, *2,3,4,5*—$\nu = h$, $\alpha = \beta = +1$, $n = 1,3,5,7$, *6*—$\nu = l$, $\alpha = \beta = +1$, $n = 0$.

$$m_n^{h\perp}(0)=m^{h\perp}_{++,n},\quad m_{S1}{}^{l\perp}(0)=m^{l\perp}_{--,0},$$

$$m_n^{h\perp}(\pi/d)=m^{h\perp}_{+-,n},\quad m_{S1}{}^{l\perp}(\pi/d)=m^{l\perp}_{-+,0}.$$

It follows from (36) that the interaction between the minibands leads to their masses vanishing at the points of the intersection $d_1 = d_{1,n}$ and to reversal of their signs after passing through zero. Near a separate intersection point we have $m^{l\perp}_{S1} = -m^{h\perp}_n$. Between the intersection points the mass $m^{l\perp}_{S1}$ reverses its sign going through infinity. The anomalously small mass of the even minibands of heavy holes, $m^{h\perp}_n \sim m_l$, $n = 1,3,5,...$, including the regions far from the intersection points $d_{1,n}$, is due to their strong interaction with the states of light holes.[7] The odd bands of heavy holes ($n = 2,4,6,...$) interact with light holes $(\varepsilon - \varepsilon_{v1})/\Lambda$ times weaker and therefore have masses of order m_{h1} for $\beta \ll 1$ (cf. Ref. 7). The d_1-dependence of the masses $m^{\nu\perp}_{\alpha\beta,n}$ calculated from (28) for the first minibands of the SL spectrum of HgTe–CdTe (see Fig. 3) confirms the qualitative analysis performed above.

The intersection of the miniband $S1$ and the minibands of heavy holes leads to the SL spectrum rearrangement with change of the structure parameters (e.g., of the potential-well widths). The evolution of the energy spectrum with d_1 changing from $d_1 < d_{1,1}(0)$ to $d_1 > d_{1,2}(\pi/d)$, e.g., when the band $S1$ crosses the bands $h1$ and $h2$, is shown in Fig. 4. In the region $d_1 < d_{1,1}(0)$ (Fig. 4a) the distance between the minibands $S1$ and $h1$ decreases drastically with increasing d_1, and the width of the SL band gap is given by the expression

$$E_g = \varepsilon^{l}_{--,0} - \varepsilon^{h}_{++,1}$$

and, decreasing with increasing d_1, it vanishes at $d_1 = d_{1,1}(0)$. The SL transforms from a direct semiconductor (Fig. 4a) to a semimetal (Fig. 4b). At the same time, according to Eqs. (28) and (36), the masses $m^{h\perp}_{++,1}$ and $m^{l\perp}_{--,0}$ vanish. Then, for $d_{1,1}(0) < d_1 < d_{1,1}(\pi/d)$ (Fig. 4b) the miniband $h1$ appears to be electronic at the center of the Brillouin zone and of hole type at the edge, for $Q = \pi/d$. The miniband $S1$, on the contrary, is of hole type at the cen-

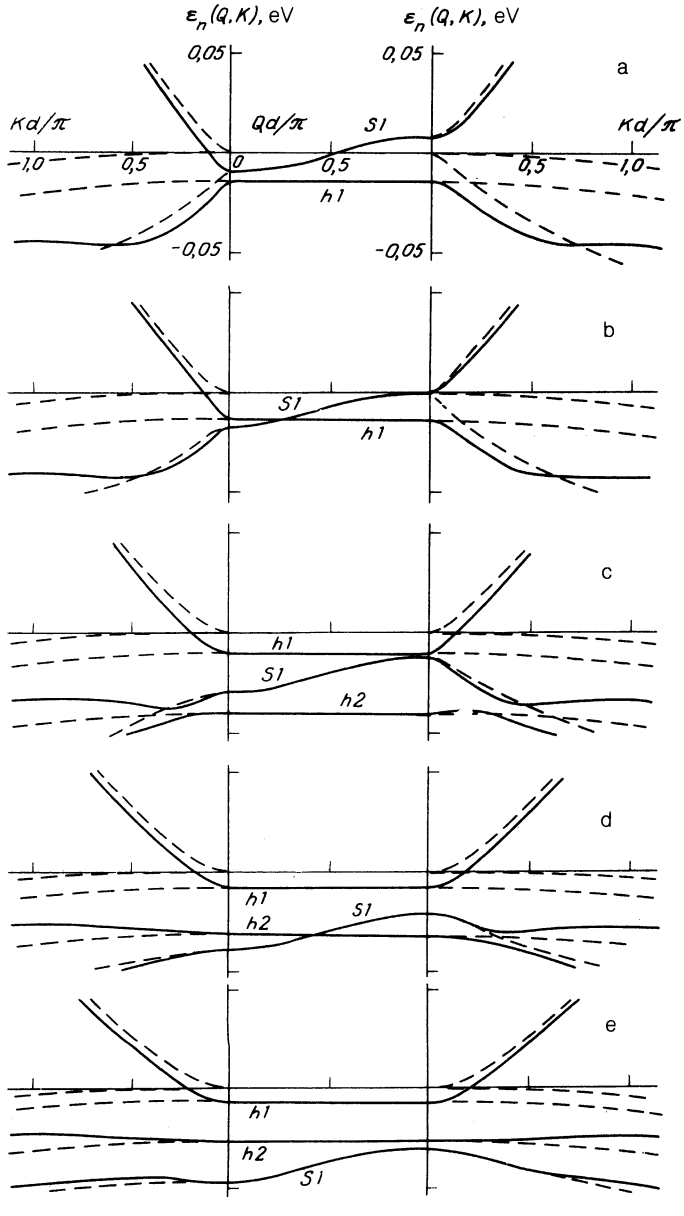

FIG. 4. The rearrangement of the energy spectrum of the carriers in the HgTe–CdTe SL with the changing thickness of the HgTe layers in the vicinity of the transition semiconductor semimetal–semiconductor for the SL parameters of Fig. 2. The dashed lines show the spectrum when the carrier transformation at the heterojunctions is not allowed for. The HgTe layers have the following thicknesses: a—66 Å $[d_1 < d_{1,1}(0)]$, b—70 Å $[d_{1,1}(0) < d_1 < d_{1,1}(\pi/d)]$, c—80 Å $[d_{1,1}(\pi/d) < d_1 < d_{1,2}(0)]$, d—90 Å $[d_{1,2}(0) < d_1 < d_{1,2}(\pi/d)]$, e—100 Å $[d_{1,2}(\pi/d) < d_1]$.

ter and electronic at the edge. For the value $Q = Q^*$ found from the equation $d_1 = d_{1,1}(Q^*)$, the masses of the minibands h 1 and S 1 reverse sign when they go through zero. The energy gap in the interval $d_{1,1}(0) < d_1 < d_{1,1}(\pi/d)$ equals zero, and the SL has the properties of a semimetal. For $d_1 > d_{1,1}(\pi/d)$ the miniband h 1 becomes electronic for all Q, and the band S 1 of hole type (Fig. 4b), the band gap is determined by the distance between them for $Q = \pi/d$, i.e.,

$$E_g = \varepsilon^h_{+-,1} - \varepsilon^l_{-+,0}$$

and increases drastically with d_1 (see Figs. 2 and 5). In the range $d_{1,1}(\pi/d) < d_1 < d_{1,2}(0)$ the SL is a direct-band semiconductor with extrema shifted to the edge $Q = \pi/d$ of the Brillouin zone.

When d_1 increases further, namely when $d_1 > d_{1,2}(0)$, the lower edge of the band S 1 crosses the second (odd) miniband of heavy holes (Fig. 4d). Due to its strong dispersion, the band S 1 experiences already in the range of small $K \sim \beta^{1/2}\pi/d_1$ a quasiintersection with the miniband h 2, so that the valence band for $K \gtrsim \pi/d_1$ coincides with the miniband h 2. Thus, the valence band appears to be strongly nonparabolic and has a second maximum for $K \approx \pi/d_1$ related to the behavior of the miniband h 2 (Fig. 4d).[3)] As d_1 grows, the top of the valence band S 1 reaches the level $\varepsilon^h_{-+,2}$, and, after their intersection for $d_1 = d_{1,2}(\pi/d)$, the valence band h 2 has only a maximum for $K \approx \pi/d_1$, so that the SL becomes an indirect-band semiconductor (Fig. 4e). Due to a small (positive) dispersion of the band h 2 for small $K \lesssim \pi/d_1$, the band gap width for $d_1 > d_{1,2}(\pi/d)$ approximately equals the distance between the bands h 1 and h 2 for $K = 0$, $Q = \pi/d$ and decreases monotonously with increasing d_1:

$$E_g \approx \varepsilon^h_{+-,1} - \varepsilon^h_{-+,2} \approx \frac{3\pi^2\hbar^2}{2|m_{h1}|d_1^2}.$$

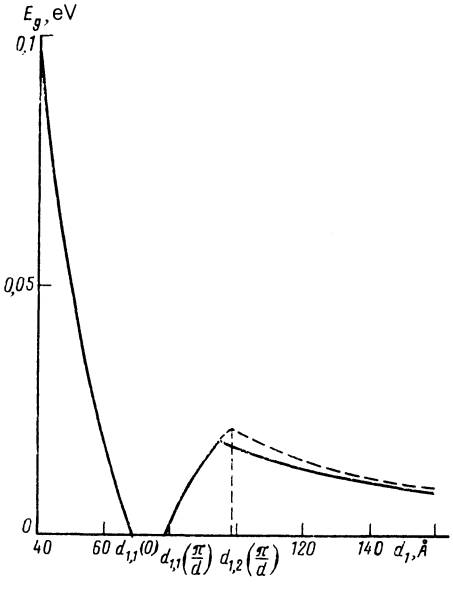

FIG. 5. The dependence of the band gap width E_g for the HgTe–CdTe SL on the width of the HgTe layers for the parameters of Fig. 2; the dashed line is the distance between the nearest c and v minibands at the point $K = 0$, $Q = \pi/d$ of the Brillouin zone.

The dependence of the band gap width in the HgTe–CdTe SL from the width of HgTe layers found with the help of the dispersion curves $\varepsilon^\nu_n(Q,K)$ obtained by solving numerically the DE (18) is shown in Fig. 5. The dashed line shows the distance between the nearest c and v minibands at the point $K = 0$, $Q = \pi/d$ of the Brillouin zone in the region, where The SL is an indirect semiconductor.

6. CONCLUSION

The DE (18) for the energy spectrum of the SL carriers obtained above allows to find the spectrum of the minibands $\varepsilon^\nu_n(Q,K)$ in a wide range of energies and momenta. The results of the calculations of the spectrum, band gap width E_g and miniband masses $m^\parallel$, $m^\perp$ agree well with the results obtained in the tight-binding approximation.[9,11] Nonmonotonic behavior of the band gap width, but depending only on the valence band discontinuity at the HgTe–CdTe interface, has been found before[8] by numerical calculations.

The rearrangement of the HgTe–CdTe SL spectrum and a related drastic decrease in hole mass for $d \approx d_{1,1}$ show in the increase in carrier mobility and the equality of the electron and hole mobilities for $d_1 \approx d_{1,1}$, as well as in their temperature dependences.[17,18]

The procedure of deriving the DE (18) shows that the structure of the miniband spectrum is determined not by the number of the bands included into the effective Hamiltonian, but by the number of the independent bulk waves important in this energy range. Thus, in the electronic region of the spectrum the single-wave approximation is valid, which can take into account not only the states of the electronic band Γ_6, but also their interaction with the states of the bands Γ_8 and Γ_7, whereas in the hole region, when the states near the bottom of the degenerate band Γ_8 are considered, the spectrum corresponds to the two-wave model. In certain ranges of the energies and material parameters (for example, when the states of the valence band in the materials with a small spin-orbit coupling are considered) the two-wave approximation may prove insufficient.

The procedure of deriving the DE (18) allows generalization to the case of propagation of N types of interacting waves ν_i, $i = 1,2,...N$. The matrix equation for the spectrum of the dimensionality $2N \times 2N$, similar to Eq. (14), reduces to a real DE including $2N - 1$ independent functions depending on the SL parameters. For a superlattice having a symmetry plane perpendicular to its axis, the DE reduces to an equation of the degree N in $\cos Qd$, in which the number of the independent functions becomes equal to N. The DE can be written in the form close in structure to the DE (18):

$$\prod_{i=1}^{N} (\cos Qd - G_{\nu i}) = \sum_{i=0}^{N-1} s_i \cos^i Qd, \qquad (37)$$

where the function $G_{\nu_i}(\varepsilon,K)$, $i = 1,2,...N$, determines the spectrum of an independent wave of the ν_i-type to the zeroth approximation and depends only on its parameters, and the right-hand side (37) gives the interaction of the waves with different ν_i. Though the explicit form of the functions $G_{\nu_i}(\varepsilon,K)$ and $s_i(\varepsilon,K)$ is determined by a specific problem, the structure of the dispersion equation (37) remains constant.

The authors are grateful to N. V. Bukhtiyarova and S. A. Martynov for performing numerical calculations.

APPENDIX

In the framework of the method of envelope functions[4,6,7] in the problem of the superlattice spectrum the parameters ε_c, ε_v, γ, $\tilde{\gamma}$ of the Hamiltonian (1) should be considered smooth functions of the coordinate x, varying from their values in the material 1 to the values in the material 2. The choice of the sequence the operators k_x, k_y, $\gamma(x)$, $\tilde{\gamma}(x)$ in the quadratic terms of the Hamiltonian (1) becoming essential. The form (1) given above corresponds to a certain choice of the model of an ideal interface discussed at length in Ref. 7. The system of equations $H\Psi = \varepsilon\Psi$ reduces to the form (2), where the matrices $D_j^{\alpha\beta}$ are given by the formulae

$$D_j^{xx} = \begin{pmatrix} A_j & C_j \\ C_j & B_j \end{pmatrix}, \quad D^{yy} = \begin{pmatrix} A_j & -C_j \\ -C_j & B_j \end{pmatrix},$$
$$D^{xy} = i\begin{pmatrix} -A_j & C_j \\ -C_j & B_j \end{pmatrix}, \quad D^{yx} = i\begin{pmatrix} A_j & C_j \\ -C_j & -B_j \end{pmatrix}, \tag{A1}$$
$$A_j = \frac{\varepsilon_P}{4(\varepsilon-\varepsilon_{cj})} - \gamma_j + \tilde{\gamma}_j, \quad B_j = \frac{3\varepsilon_P}{4(\varepsilon-\varepsilon_{cj})} - \gamma_j - \tilde{\gamma}_j,$$
$$C_j = 3^{1/2}\left(\frac{\varepsilon_P}{4(\varepsilon-\varepsilon_{cj})} - \tilde{\gamma}_j\right).$$

The boundary conditions are obtained by integrating the system $\hat{H}\Psi = \varepsilon\Psi$ over the region near the interface, which gives

$$\Psi|_{-0}^{+0} = 0, \quad \sum_{\alpha=x,y} D_j^{x\alpha} k_\alpha \Psi|_{-0}^{+0} = 0, \tag{A2}$$

where $f|_{-0}^{+0}$ is the discontinuity of the function f at the interface. The relations (A2) give the linear relation between the coefficients C_{lj} of the superposition determining the wave functions in the materials 1 and 2. This allows to find the explicit expressions for the elements of the matrix R from (8):

$$R_{11} = \frac{1}{2}\left(\frac{k_{h2}}{k_{h1}} + \frac{\varepsilon-\varepsilon_{v2}}{\varepsilon-\varepsilon_{v1}} - \frac{iK}{2k_{h1}}\frac{\Lambda}{\varepsilon-\varepsilon_{v1}}\right),$$
$$R_{12} = \frac{1}{2}\left(-\frac{k_{h2}}{k_{h1}} + \frac{\varepsilon-\varepsilon_{v2}}{\varepsilon-\varepsilon_{v1}} - \frac{iK}{2k_{h1}}\frac{\Lambda}{\varepsilon-\varepsilon_{v1}}\right), \tag{A3}$$
$$R_{13} = R_{14} = -i\frac{3^{1/2}}{4}\frac{K}{k_{h1}}\frac{\Lambda}{\varepsilon-\varepsilon_{v1}}.$$

The elements R_{2m} are obtained from the elements R_{1m} by the substitution $k_{h1} \to -k_{h1}$, the elements R_{lm}, $l,m = 3,4$ from the elements $R_{l-2,m-2}$ by the substitution $k_{hj} \to k_{lj}$ and $K \to -K$, and, finally, the elements R_{lm}, $l = 3,4$, $m = 1,2$, from the elements $R_{l-2,m+2}$ by the substitution $k_{h1} \to k_{l1}$.

[1)] A detailed discussion of this method, as well as of the boundary conditions at the heterojunction, is contained in Ref. 3.
[2)] In the adopted miniband enumeration there is a relation between the values α and n: for the miniband originating from the nth level of the size quantization $\alpha = (-1)^{n+1}$.
[3)] The dispersion of the miniband $h2$ and, in particular, the maximum appearing for $K \approx \pi/d_1$ have been discussed in detail in Ref. 7.

[1] A. P. Silin, Usp. Fiz. Nauk **147**, 485 (1985) [Sov. Phys. Usp. **28**, 972 (1985)].
[2] G. Bastard and J. A. Brum, J. Quantum Electron. **QE-22**, 1625 (1986).
[3] D. L. Smith and C. Mailhiot, Rev. Mod. Phys. **62**, 173 (1990).
[4] G. Bastard, Phys. Rev. B **25**, 7584 (1982).
[5] M. I. Dyakonov and A. V. Khaetskiĭ, Zh. Eksp. Teor. Fiz. **82**, 1584 (1982) [Sov. Phys. JETP **55**, 917 (1982)].
[6] R. A. Suris, Fiz. Tekh. Poluprovodn. **20**, 2008 (1986) [Sov. Phys. Semicond. **20**, 1258 (1986)].
[7] L. G. Gerchikov and A. V. Subashiev, Phys. Status Solidi B **160**, 443 (1990).
[8] N. F. Johnson, P. M. Hui, and H. Ehrenreich, Phys. Rev. Lett. **61**, 1993 (1988).
[9] C. A. Hoffman, J. R. Mayer, and F. G. Bartoli, Phys. Rev. B **38**, 12457 (1988).
[10] C. A. Hoffman, J. R. Mayer, and F. J. Bartoli, Phys. Rev. B **40**, 3867 (1989).
[11] J. N. Schulman and Y. C. Chang, Phys. Rev. B **33**, 2594 (1986).
[12] M. Altarelli, Phys. Rev. B **28**, 842 (1983).
[13] F. G. Bass, A. A. Bulgakov, and A. P. Teterevov, *High Frequency Properties of Semiconductors with Superlattices* [in Russian] Nauka, Moscow, 1989.
[14] F. R. Gantmakher, *Theory of Matrices* [in Russian], Nauka, Moscow, 1988.
[15] A. M. Cohen and G. E. Marques, Phys. Rev. B **41**, 10608 (1990).
[16] J. M. Berroir, Y. Guldner, J. P. Vieren, M. Voos, and J. P. Faurie, Phys. Rev. B **34**, 891 (1986).
[17] J. R. Mayer, C. A. Hoffman, F. J. Bartoli *et al.*, Phys. Rev. B **38**, 2204 (1988).
[18] C. A. Hoffman, J. R. Mayer, F. J. Bartoli *et al.*, Phys. Rev. B **39**, 5208 (1989).

Translated by E. Khmelnitski